

NMR IMAGING APPLICATION TO CARBON DIOXIDE MISCIBLE FLOODING IN WEST TEXAS CARBONATES

R. D. Hazlett, J. W. Gleeson,* H. Laali, and R. Navarro
Mobil Research and Development Corporation
Mobil Exploration and Producing Technical Center
13777 Midway Rd., Dallas, TX 75244
*Paulsboro Research Laboratory
Paulsboro, NJ

ABSTRACT

The median Nuclear Magnetic Resonance (NMR) relaxation time was previously shown to be strongly correlated to laboratory carbon dioxide miscible flood displacement efficiency in San Andres crystalline dolomite cores. According to a pore size interpretation of relaxation times, samples of smaller median pore size were more efficiently swept. Such a correlation was not observed for a number of Wolfcamp limestone samples. In order to study displacement mechanisms, information on sample heterogeneity and residual oil distribution was needed. NMR images of the end-point oil concentration distribution were taken following gravity stable, CO₂ core floods on selected specimens. NMR porosity and relaxation time images were acquired on the same clean, fully water saturated samples to demonstrate the relationship between relaxation time spatial distribution, flow barriers, and residual oil distribution. Bypassing was confirmed to be the major mechanism of residual oil stranding. Pore size proved to be a good measure of sample heterogeneity in the case of crystalline dolomite probably because of diagenetic homogenization. For the Wolfcamp limestone, other types of heterogeneity were observed such as laminations, bioturbation, or diagenetic fabric which caused the median pore size to be a poor indicator of displacement performance. These results were supported by a limited number of in-situ polymerization experiments. In all cases examined, heterogeneity on the core level could explain trends with respect to laboratory CO₂ miscible flood displacement efficiency and residual oil saturation distribution.

INTRODUCTION

Microscopic displacement efficiency is a concern even in miscible flooding as continuous, unobstructed pathways must exist in porous matrix to allow for oil contact, mobilization, and recovery¹. The high interpore connectivity in sandstones usually yields high recovery efficiencies, but more complex carbonate systems can display significant remaining oil saturations following CO₂ laboratory displacements². Since current CO₂ flooding operations involve predominantly carbonate-based systems, some predictive ability is desired for operational strategies and expansion opportunities. Knowledge of the rock fabric or diagenetic characteristics responsible for phase trapping and a method to estimate the extent of those features in geologic sections would lead to such a predictive tool.

NMR relaxation was found to strongly correlate with the remaining oil saturation following gravity stable laboratory core displacements above the minimum miscibility pressure in San Andres dolomite samples from West Texas³. Interpretation of those results suggested more oil was recovered in samples with a smaller median pore size. It was claimed that the evidence of larger pores coincided with wider pore size distributions, hence heterogeneity. It was desired to know not only the oil saturation endpoint, but also how the unrecovered oil was distributed within the core, especially with respect to geological features. NMR imaging allowed

investigation of oil distributions, porosity distribution, and a measure of porosity domain size distributions. These investigations are needed to support or reject hypotheses with regard to displacement mechanisms and mode of residual oil stranding.

Use of miscible flood microscopic displacement efficiency core tests to predict reservoir behavior requires a tie into information available in logs or geologic sections. Bulk porosity and permeability values were found to be inadequate indicators of performance^{3,4}. For reservoir rock types in which NMR relaxation correlates with displacement efficiency, the advanced NMR logging tools may allow distribution of predicted endpoint saturations. In the absence of such a correlation, an alternative methodology was examined for cored well intervals.

An in-situ polymerization procedure was also developed to allow isolation and identification of pore level features responsible for phase trapping, as well as core-scale quantification of the residual oil under miscible conditions. Subsequent visualization and direct comparison of the both the trapping and non-trapping pore network elements enables assessment of the controlling factors for recovery efficiency. Identification of the pores responsible for entrapment of the residual oil and association with certain obvious geologic features allows correlation between geology and residual oil distribution for larger than core scale reservoir characterization. In-situ polymerization and NMR imaging are complementary procedures.

METHODS AND PROCEDURES

Sample Selection

Wolfcamp core samples covering a broad spectrum of porosity and permeability characteristics from coarsening upward calcarenite sequences of carbonate shoal facies were selected. Two-inch diameter cores plugs were obtained at each selected depth. Samples were cleaned and dried prior to use. End pieces were retained for NMR relaxation studies to complement previous work with San Andres crystalline dolomite³.

Nuclear Magnetic Resonance Relaxation

Irregularly shaped end pieces from one inch Wolfcamp core plugs were chemically extracted, cleaned, dried, and weighed. The rock pieces were prepared for NMR relaxation as before³. A Bruker Minispec P-10, which operates at 10MHz, was used to construct standard inversion-recovery curves. Relaxation time distributions were obtained from NMR relaxation data by a Laplace inversion method which seeks continuous distribution functions. In this manner, relaxation information on a bulk sample was obtained, and a deconvolution procedure subdivided the signal into a distribution of components. Similar measurements, however, were made locally, producing relaxation time images as described in the forthcoming sections.

Core flooding

Core floods were carried out as gravity stable displacements with 1600 psi backpressure in the absence of water using live crude oil and hydrocarbon enriched CO₂. Procedures were the same as those outlined previously^{3,5}. A schematic of the experimental setup is shown in Figure 1. Floods were discontinued at gas-oil ratio (GOR) of 60,000. The core holder was then isolated from the rest of the system and allowed to cool to room temperature. A metering valve was attached to the outlet, and the internal core pressure was slowly released. The exhaust gas was bubbled through a liquid-filled beaker to monitor the rate of expansion.

NMR Imaging

A sequence of core handling steps was followed to provide NMR images of the resulting oil distribution, the porosity, and relaxation times. A depressurized sample was removed from the Hassler cell and wrapped in Saran[®] wrap. The core was centered within a 40 cm bore, 50 MHz Bruker horizontal magnet. Three-dimensional NMR images of the remaining hydrocarbon distribution were taken at 1 mm resolution using a pulsed gradient technique with 1 second recovery time. The core was then removed and a soxhlet solvent extraction method was used to recover remaining oil. Solvent extraction was repeatedly performed with pure toluene until the solvent returned to its original clear color. Residual oil was computed by weight loss after drying.

The cleaned core was resaturated with deaired water, wrapped to avoid evaporation loss, and placed in a sealed container for imaging. Three-dimensional images were obtained at five different sampling times for construction of relaxation time images for selected samples. The longest recovery time image at four seconds also represented the full porosity map. Relaxation time images were computed using a single exponential decay model on a voxel by voxel basis. For voxels where signal-to-noise was deemed poor, voxel values were masked to zero.

In-Situ Polymerization

The apparatus for in-situ polymerization studies is shown in Figure 2. Selected cleaned and extracted dry core samples were mounted in the Hassler cell assembly and saturated with blue-dyed (CIBA-GEIGY Oracet Blue 2R) styrene at 1200 psi back pressure. Blue styrene was injected at 5 cc/hr while obtaining baseline readings on the spectrophotometer. Red-dyed (CIBA-GEIGY Oracet Red G) styrene was then injected to displace the blue-dyed styrene. An initiator, free radical generator 1,1'-azobis (cyclohexanecarbonitrile) obtained from DuPont as VAZO 88, is added to the styrene monomer as well to aid rapid polymerization. A computer interfaced with the spectrophotometer recorded the effluent dye absorption. Absorption levels were translated into red and blue fractions from prior calibration procedures. The resulting normalized effluent concentration versus pore volumes of injected styrene allows characterization of dispersion and an estimation of the unrecovered fraction. At roughly one pore volume of injection, flow was halted. The core sample was removed and rapidly polymerized through application of heat. The polystyrene impregnated rock was then sliced and examined visually. The dyes aid delineation of both flowing and stagnant pore spaces. Appropriate parts were also thin-sectioned for petrographic examination and association of the residual phase (blue dye) with obvious geologic features.

RESULTS

NMR Relaxation

Core properties, displacement results, and NMR relaxation times are listed in Table 1. The NMR relaxation results for the Wolfcamp samples are plotted along with the San Andres data in Figure 3. The mean relaxation time was not found to be a good indicator of miscible displacement performance in the limestone samples tested. More extensive testing of carbonate rocks with varying pore attributes and grades was deemed necessary to establish correlations between rock texture and displacement efficiency.

NMR Imaging

NMR imaging results are documented herein for three different cores exhibiting different behavior. Figure 4 displays images of porosity, remaining oil concentration distribution, and relaxation time for Sample 6. The relaxation time images were found to contain the range from

0.25-3 seconds with a mean of about 1 second and were highly correlated with porosity images. This sample shows pronounced thin laminations across the entire core plug length. The inclined low porosity laminations seem to shield parts of the core from being effectively swept. A second streak of relatively high oil concentration was observed adjacent to but separated from the major low porosity feature. A connection between the porosity mapping and the oil concentration was not obvious for this volume element. Evidence of layering in this region was not apparent from visual observation. However, the relaxation time image clearly indicates this to be a continuous layer of lower relaxation time. In this instance, the T_1 image suggests the oil was bypassed due to permeability contrast rather than through shielding by low porosity features. Low-power petrographic observations indicate that although laminations are caused by alternating coarse and fine carbonate grains, the lamina with the coarse grains also selectively host more diagenetic cement. This selectively causes lower permeability in the lamina containing coarser grains.

Figure 5 contains porosity and remaining oil concentration distribution image slices from Sample 7. In Sample 7, rather large, irregularly shaped structures were present which again strongly biased the fluid displacement process. Three-dimensional examination of the data indicated a relationship between the spatial arrangement of low porosity features and the remaining oil concentration distribution. These effects are not particularly evident in examination of single two dimensional slices. Particular image features suggested bioturbation. Petrographic observations indicate that low porosity areas correspond to higher levels of diagenetic cementation.

As seen in Figure 6, Sample 10 was found to strand oil in small, seemingly disconnected clusters. This particular orientation of remaining oil was the most commonly observed in the cores tested. A low porosity angular structure near the outlet was seen to severely alter the remaining oil distribution profile. Low-power petrographic observations indicate that fusulinid foraminifera tests are abundant and resemble distribution of both the porosity and residual oil anomalies.

Wolfcamp limestone core samples examined from a single cored interval clearly showed a variety of heterogeneities. Core sweep patterns were found to be strongly governed by structures observable in NMR images rather than pore scale features. In general, high oil concentrations were found associated with the downstream side of low porosity features. Often residuals increased towards the outlet. In all cases, remaining oil distributions were correlatable to heterogeneities observable from 1 mm^3 resolution images, although the geologic origin of the heterogeneities required further examination.

In-Situ Polymerization

One core (Sample 4) which was polymerized and slabbed after approximately one pore volume throughput of red-dyed styrene is shown in Figure 7. The blue-dyed regions indicate undisplaced styrene. The core shows a rather dramatic patch-like arrangement of well and poorly swept domains. Microscopic examination of the rock reveals that the residual phase is trapped in early marine, fine-textured diagenetic cement. It is proposed that nonuniform early cementation influenced subsequent diagenetic dissolution / precipitation patterns to yield an array of poorly connected domains within higher connectivity matrix.

In addition, the unrecovered styrene was commonly associated with foraminifer fossils, which appear as rounded or oval features in Figure 7. Figure 8 shows a digital photomicrograph of styrene stranding within foram fossil chambers. Such porosity features were penetratable but may not contain a discernable "inlet" and "outlet" for efficient displacement along a predetermined direction. Some fossils were also found in the well-swept regions -- but to a

lesser extent. The discontinuous, oval-shaped bright spots in many of the NMR images of the remaining oil saturation, such as Figure 6, could now be associated with the abundance of foraminifera.

It has not been shown that early marine cementation and foraminifera abundance are the sole causes for poor microscopic displacement efficiency within the Wolfcamp, but they are concrete examples where known diagenetic and depositional features are observed responsible for development of flow patterns on the core scale. The early cementation diagenetic products can be readily observed in polished core slabs and thin-sections of the grainstone shoal facies. In-situ polymerization also allows examination of attributes at the pore scale with the aid of light and electron microscopy. This procedure, therefore, allows application of results of microscopic sweep efficiency to larger than core scale intervals of the reservoir rock.

CONCLUSIONS

- Remaining oil saturations following gravity stable CO₂ miscible displacement in Wolfcamp limestone core samples tested were relatively large (>15%).
- NMR imaging clearly shows heterogeneities on the core scale and provides a tool for assessment of the controlling factors of displacement.
- Although NMR relaxation may serve as a measure of heterogeneity and residual oil for rocks characterized by diagenetic homogenization (San Andres dolomites), it fails in the presence of pore network heterogeneities, such as those for Wolfcamp Limestone.
- In the limestone cores investigated, remaining oil saturation distributions following a CO₂ miscible displacement of crude oil were visually correlated to the presence of low porosity or permeability features.
- In-situ polymerization procedures clearly shows areas of entrapment and strongly suggest the association of stranded oil with the patterns of early marine cementation and micropores associated with fusulinid foraminifera tests in the Wolfcamp limestone.
- Features observable in NMR imaging could be associated with the geology through core examination and miscible styrene displacements.
- The combination of NMR imaging and in-situ polymerization allowed identification of bypassing as a primary mode of residual oil stranding in Wolfcamp limestone cores examined and suggested the means for extrapolating laboratory core flood data through use of core records.
- The large variety of structures observed in Wolfcamp limestone increases the number of core studies necessary to draw statistically significant conclusions with regard to displacement efficiency on the reservoir scale.

ACKNOWLEDGEMENTS

Thanks to Mary Jane Furr for performing the NMR relaxation experiments, Don Woessner for his contributions, and Hai Nguyen, Amy Vanderhill, and Matt Honapour for their interest and feedback.

REFERENCES

1. Stalkup, F. I. Jr.: Miscible Displacement, Society of Petroleum Engineers of AIME, Monograph Vol. 8, New York (1984) 55-62.
2. Spence, A. P. and Watkins, R. W.: "The Effect of Microscopic Core Heterogeneity on Miscible Flood Residual Oil Saturation," paper SPE 9229 presented at the 55th Annual Fall Technical Conference and Exhibition, Dallas, September 21-24, 1980.
3. Hazlett, R. D., Furr, M. J., and Navarro, R.: "A Correlation for Miscible Flood Displacement Efficiency in the San Andres with NMR Relaxation," paper SPE 23992 presented at the Permian Basin Oil and Gas Recovery Conference, Midland, March 18-20, 1992.
4. Bilhartz, H. L. Jr. and Charlson, G. S.: "Coring for In-Situ Saturations in the Willard Unit CO₂ Flood Mini-Test," paper SPE 7050 presented at the Fifth Symposium on Improved Methods for Oil Recovery, Tulsa, April 16-19, 1978.
5. Watkins, R. W.: "A Technique for the Laboratory Measurement of Carbon Dioxide Unit Displacement Efficiency in Reservoir Rock," paper SPE 7474 presented at the 53rd Annual Fall Technical Conference and Exhibition, Dallas, October 1-3, 1978.

Table 1. Properties of Wolfcamp limestone cores in this study.

Sample No.	Depth [ft]	Porosity ϕ	Permeability [md]	End-Point Saturation	T ₁ ^{50%} [msec]
1	9052.1	9.8	1.03	16.3	
2	9083.0	-	-	-	250
3	9125.0	-	-	-	625
4	9139.2	19.0	175	19.0	250
5	9212.0	-	-	-	714
6	9212.9	12.9	0.81	25.8	709
7	9216.1	14.8	6.7	22.3	250
8	9223.5	10.4	0.40	15.1	243
9	9223.7	10.1	0.40	25.1	147
10	9284.1	5.9	0.17	17.9	251
11	9311.0	-	-	-	555
12	9335.0	-	-	-	125

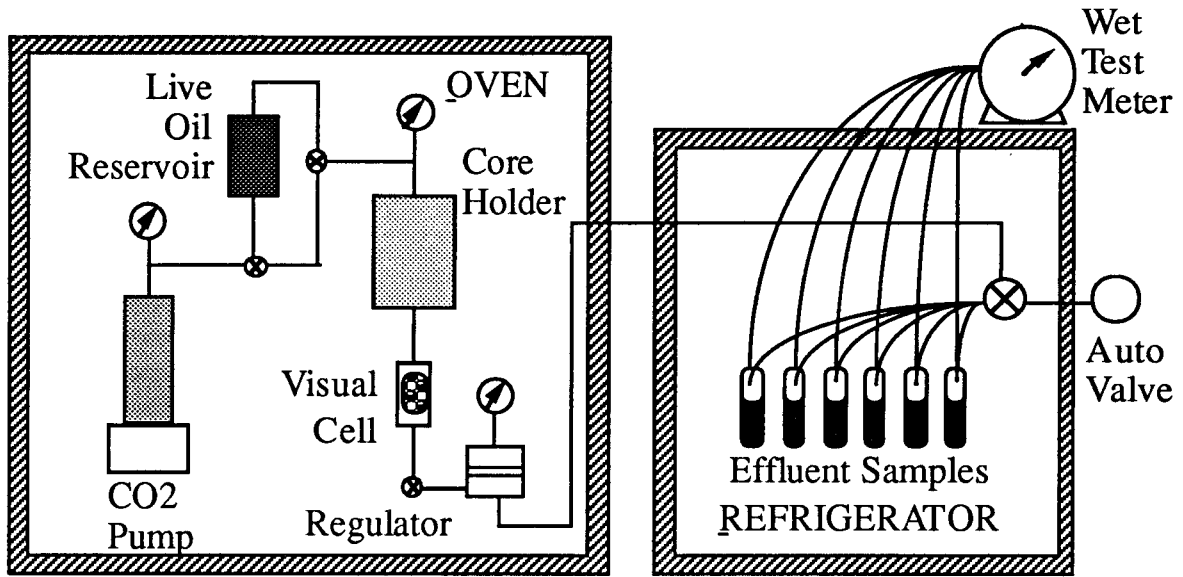


Figure 1. Schematic for gravity-stable CO₂ coreflood experiments.

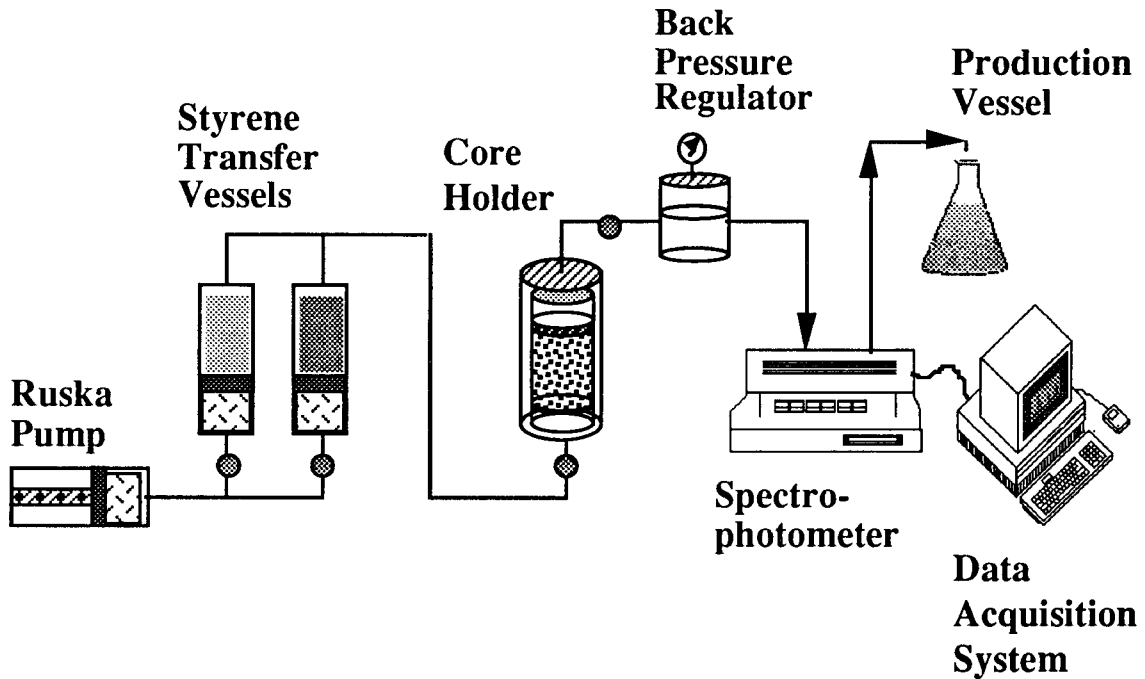


Figure 2. Identifying "culprit" pore elements.

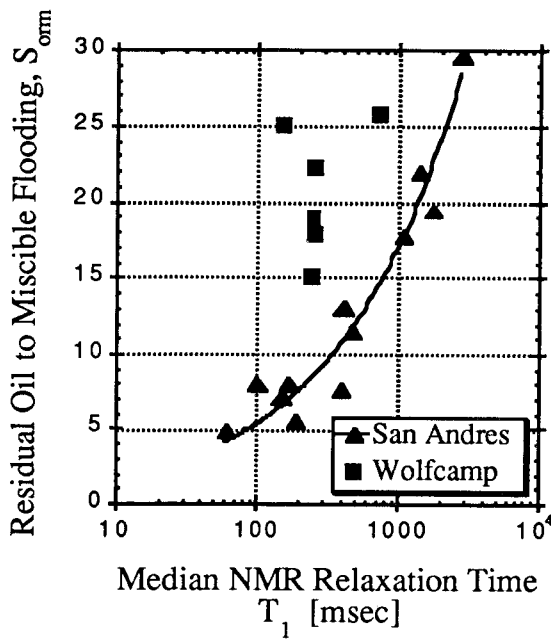


Fig. 3. NMR relaxation time and carbon dioxide miscible coreflood efficiency.

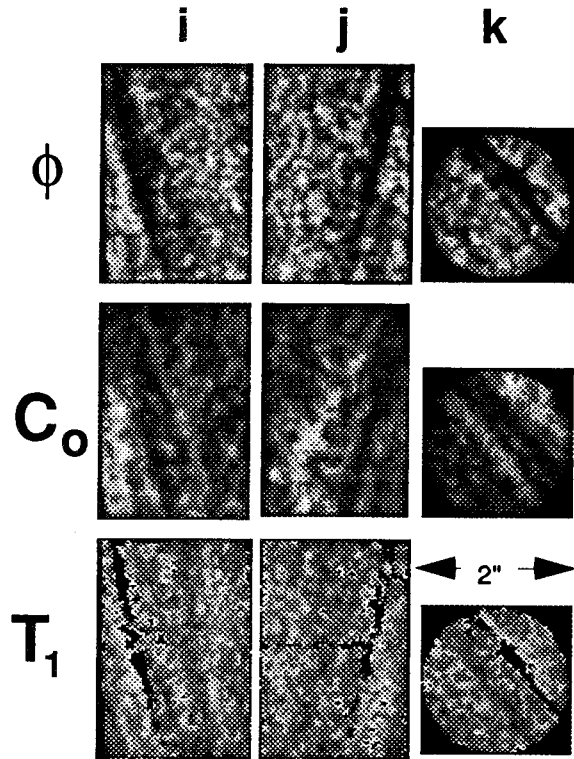


Fig. 4. Central orthogonal NMR images of Sample 6: porosity, oil concentration, and spin-lattice relaxation time [light = high].

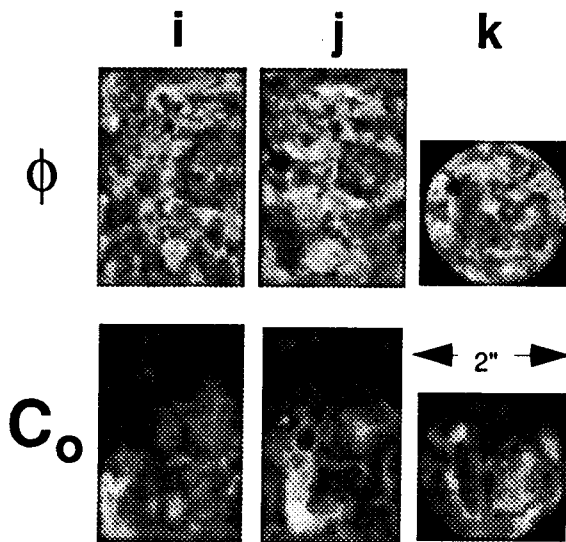


Fig. 5. Central orthogonal NMR images of Sample #7: porosity and oil concentration [light = high].

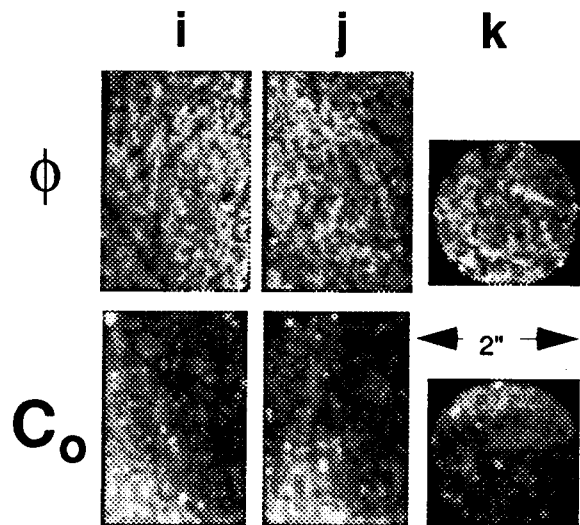


Fig. 6. Central orthogonal NMR images of Sample #10: porosity and oil concentration [light = high].



Fig. 7. Slabbed Wolfcamp core #4 following a red displacing blue styrene flood.

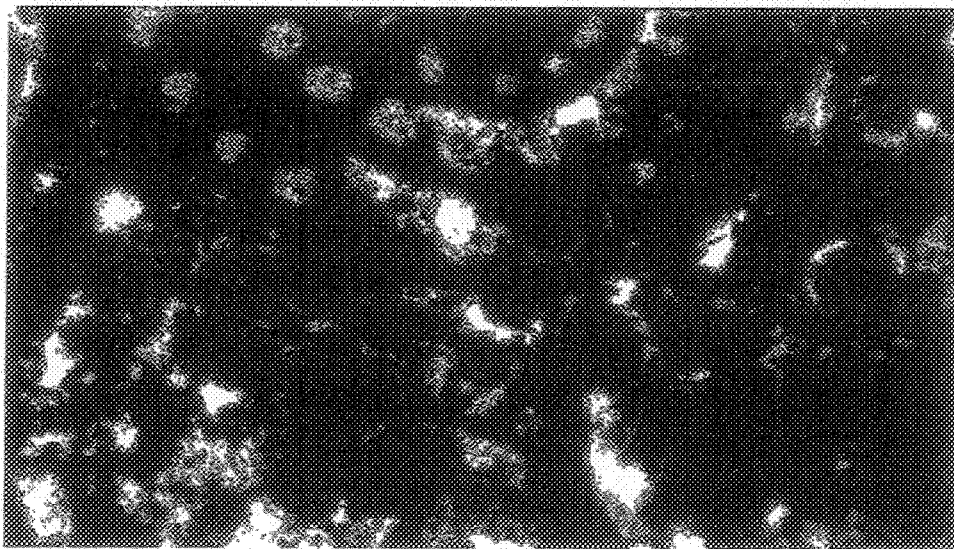


Fig. 8. Foraminifer fossil showing blue styrene entrapment.

